Am J Physiol Lung Cell Mol Physiol 283: L766–L776, 2002.
First published May 3, 2002; 10.1152/ajplung.00250.2000.

γ-Glutamyl transferase deficiency results in lung oxidant stress in normoxia

JYH CHANG JEAN,[1] YUE LIU,[1] LOU ANN BROWN,[2] ROBERT E. MARC,[3] ELIZABETH KLINGS,[1] AND MARTIN JOYCE-BRADY[1]
[1]*Pulmonary Center at Boston University School of Medicine, Boston, Massachusetts 02118;*
[2]*Department of Pediatrics, Emory University, Atlanta, Georgia 30322; and*
[3]*Moran Eye Center, University of Utah, Salt Lake City, Utah 84108*

Received 27 July 2000; accepted in final form 30 April 2002

Jean, Jyh Chang, Yue Liu, Lou Ann Brown, Robert E. Marc, Elizabeth Klings, and Martin Joyce-Brady. γ-Glutamyl transferase deficiency results in lung oxidant stress in normoxia. *Am J Physiol Lung Cell Mol Physiol* 283: L766–L776, 2002. First published May 3, 2002; 10.1152/ajplung.00250.2000.—γ-Glutamyl transferase (GGT) is critical to glutathione homeostasis by providing substrates for glutathione synthesis. We hypothesized that loss of GGT would cause oxidant stress in the lung. We compared the lungs of GGT^{enu1} mice, a genetic model of GGT deficiency, with normal mice in normoxia to study this hypothesis. We found GGT promoter 3 (P3) alone expressed in normal lung but GGT P3 plus P1, an oxidant-inducible GGT promoter, in GGT^{enu1} lung. Glutathione content was barely decreased in GGT^{enu1} lung homogenate and elevated nearly twofold in epithelial lining fluid, but the fraction of oxidized glutathione was increased three- and fourfold, respectively. Glutathione content in GGT^{enu1} alveolar macrophages was decreased nearly sixfold, and the oxidized glutathione fraction was increased sevenfold. Immunohistochemical studies showed glutathione deficiency together with an intense signal for 3-nitrotyrosine in nonciliated bronchiolar epithelial (Clara) cells and expression of heme oxygenase-1 in the vasculature only in GGT^{enu1} lung. When GGT^{enu1} mice were exposed to hyperoxia, survival was decreased by 25% from control because of accelerated formation of vascular pulmonary edema, widespread oxidant stress in the epithelium, diffuse depletion of glutathione, and severe bronchiolar cellular injury. These data indicate a critical role for GGT in lung glutathione homeostasis and antioxidant defense in normoxia and hyperoxia.

glutathione; heme oxygenase-1; 3-nitrotyrosine

EXTRACELLULAR GLUTATHIONE metabolism is initiated by the key enzyme γ-glutamyl transferase (GGT) and then completed by membrane dipeptidases. The released amino acids, particularly cysteine, serve as essential substrates for intracellular glutathione and protein synthesis. Genetic GGT deficiency in the GGT^{enu1} mouse impairs glutathione metabolism and transport and results in systemic glutathionemia, glutathionuria, and oxidant stress in the kidney (15, 19). GGT expression is low in the lung compared with other tissues such as the kidney, epididymis, and pancreas (1, 37). Hence, it is not certain that GGT deficiency would produce an oxidant stress in this organ. The low level of lung GGT activity is believed to contribute to an abundance of glutathione in the lung epithelial lining fluid (ELF) (4, 8).

Our previous studies have shown that the GGT gene is expressed in distal lung epithelium and that enzymatically active GGT protein is present in lung surfactant (22). Exposure to an inhaled oxidant (NO_2) induces GGT gene expression within the epithelium and GGT protein accumulation within surfactant, implying an active role for GGT-mediated glutathione metabolism at the epithelial surface of the lung (36). Thus we predict that a loss of this activity will impair glutathione homeostasis at this surface and predispose to injury by inhaled oxidants. To study this, we previously characterized the point mutation that inactivated GGT expression in the GGT^{enu1} mouse and developed a strategy to breed and genotype this model of GGT deficiency. We compare normal (wild-type, +/+) with GGT^{enu1} (mutant, −/−) mice for the presence of oxidant stress in 21% O_2 based on the pattern of GGT mRNA expression, lung glutathione content, and redox ratio and reactivity for 3-nitrotyrosine residues by immunocytochemistry and then test their ability to survive in >95% O_2. Our results establish an important role for GGT in protecting the distal lung against oxidant stress in normoxia and hyperoxia.

METHODS

Breeding. The GGT^{enu1} mouse was bred and housed in the Laboratory and Animal Science Center at Boston University School of Medicine according to approved guidelines. Hemizygous pairs were mated, and offspring were genotyped at 4 wk of age using tail-derived DNA and direct sequencing of PCR products as described elsewhere (19). Animals were fed Purina mouse chow and allowed access to water ad libitum.

RT-PCR. Lung RNA was obtained from wild-type and mutant mice using Tri-reagent. The RT reaction and the primary and secondary PCRs were performed as described by

Address for reprint requests and other correspondence: M. Joyce-Brady, The Pulmonary Center, 715 Albany St., R304, Boston, MA 02118 (E-mail: mjbrady@lung.bumc.bu.edu).

The costs of publication of this article were defrayed in part by the payment of page charges. The article must therefore be hereby marked "*advertisement*" in accordance with 18 U.S.C. Section 1734 solely to indicate this fact.

Joyce-Brady et al. (22). Primers used to target rat GGT promoters P1, P2, and P3 were modified for mouse GGT P1, P2, and P3 on the basis of the published mouse GGT cDNA sequences (35). Products were separated on 1.5% agarose gels along with DNA standards, visualized after staining with ethidium bromide, and photographed under ultraviolet light. Kidney RNA obtained from normal mice served as a positive GGT mRNA control, since all three GGT mRNA subtypes are expressed in this organ (31). Results were compared with normal rat lung.

Glutathione assay. The lung was perfused with PBS, lavaged with 0.5 ml of PBS, and frozen in liquid nitrogen. Tissue (50–100 mg) was combined with 5% perchloric acid by trituration for 30 s on a liquid nitrogen bath. Insoluble material was pelleted by centrifugation at 5,000 *g* for 5 min at 4°C. The number of cells obtained from lung lavage was determined on a Coulter counter. An aliquot was used for cytospin preparations to determine cellular composition after Wright stain, and the remaining cells were collected by centrifugation at 1,000 *g* for 10 min at 4°C and extracted in 5% perchloric acid. The supernatant was combined with an equal volume of ice-cold 10% perchloric acid, and insoluble material was pelleted by centrifugation. All samples were frozen in liquid nitrogen, stored in aluminum foil at −70°C, and assayed within 1–3 days.

Total glutathione was measured using the recycling method of Teitze as described by Rishikoff et al. (33). Standard curves were constructed using known concentrations of glutathione run in parallel with lung samples in a multiwell plate. The reaction was incubated for 5 min, and absorbance was measured at 405 nm on a plate reader (Molecular Devices, Menlo Park, CA). Tissue glutathione is expressed as nanomoles per milligram of protein, cellular glutathione as nanomoles per 10^6 cells, and plasma plus lavage fluid as micromolar, with the lavage concentration being corrected by the urea dilution method (32). Urea nitrogen was determined with a quantitative enzymatic end-point assay kit (Sigma Diagnostics, St. Louis, MO). Five microliters of lavage fluid or plasma were assayed in 1 ml of reagent buffer, the reaction was incubated for 5 min, and absorbance was measured at 340 nm on a Beckmann spectrophotometer. Because the glutathione content of cells in the lavage fraction was below the detectable limit of our assay, HPLC was used for the assay, as described by Bai et al. (2). HPLC was also used to determine the fraction of oxidized glutathione (GSSG) in lung, lung lavage fluid, and lavage cells.

An immunohistochemical method was used to assess glutathione content in airway epithelial cells in situ. Lung and liver tissues were perfusion fixed with 1% paraformaldehyde and 2.5% glutaraldehyde at room temperature, excised and immersed in the same fixative, and immediately transferred to the laboratory of Dr. Robert Marc, where they were embedded in epoxy resin (Eponate 812), sectioned at 250 nm, and processed for standard high-performance immunocytochemistry with silver visualization, as described elsewhere (25). Data were acquired from serial 250-nm sections from a composite block containing normal and GGT^{enu1} liver or lung tissue. Glutathione was probed with Signature Immunologics J100 IgG. Normal and GGT^{enu1} tissues were probed in the same 25-ml droplet and visualized with silver-intensified immunogold detection using a 4-min development time at 30°C. Glutathione signal specificity was ensured in competition assays by coincubation of antibody with 250 μM reduced glutathione.

Immunohistochemistry for 3-nitrotyrosine. Peroxynitrite production was assessed as a marker of oxidant stress in lung tissue by immunoassay for 3-nitrotyrosine. Tissue sections were deparaffinized, and endogenous peroxides were quenched with 3% H_2O_2 in methanol. Some sections were incubated with 1 mM exogenous peroxynitrite for 10 min to serve as a positive control. All sections were blocked with 8% BSA for 30 min before addition of a 4 μg/ml solution of the polyclonal rabbit α-nitrotyrosine antiserum (catalog no. 06-284, Upstate Biotechnology, Lake Placid, NY) for 1 h at room temperature. Nonimmune serum was used in this incubation step for the negative control. Competition experiments were performed using 10 mM nitrotyrosine to ensure specificity of the nitrotyrosine signal. Reactivity was detected using a goat α-rabbit IgG antibody coupled to 3,3′-diaminobenzidine (DAB) peroxidase (Vector Laboratories) with DAB as substrate.

Exposure to hyperoxia. Mice were exposed to an atmosphere of >95% O_2-balance N_2 (Wesco Gases, Billerica, MA) by enclosing their cages in an airtight glove bag. O_2 concentration was continuously monitored by oximetry. Crystalit absorption medium (Pharmacal, Naugatuck, CT) was added to bedding at 10 g/ft^2 of cage. Drierite (Vacumed, Ventura, CA) and Sodasorb (Intertech Resources, Lincolnshire, IL) were dispersed throughout the glove bags to absorb water and CO_2. Animals were checked for viability every 6 h. Lung tissues from wild-type and mutant mice were fixed with paraformaldehyde, embedded in paraffin, sectioned, stained with hematoxylin and eosin, and examined as described previously (29).

In additional experiments, normal ($n = 3$) and GGT^{enu1} ($n = 3$) mice were exposed to hyperoxia for 96 h and then tissues were processed for histology, heme oxygenase-1 (HO-1) expression, and glutathione immunohistochemistry. HO-1 was examined in lung tissue by immunohistochemistry using a 1:25 dilution of a mouse monoclonal antibody (IgG2b) that was raised against the intact rat HO-1 protein (catalog no. OSA-111, StressGen Biotechnologies, Victoria, BC, Canada) as the primary antibody together with the mouse-on-mouse kit (MOM kit, Vector Laboratories) and a horseradish peroxidase-conjugated secondary antibody with DAB as substrate. Primary and secondary antibodies were omitted separately and together as negative controls.

HO-1 protein was also assessed on a Western blot. Lung total proteins were extracted with 150 mM NaCl, 0.5% deoxycholate, 1% NP-40, 0.1% SDS, and 50 mM Tris (pH 7.6), separated on a 10% SDS-polyacrylamide gel along with protein standards, and electroblotted onto a nitrocellulose filter (Optitran, Schlicher & Schuell, Keene, NH). The filter was probed for HO-1 protein using a 1:1,000 dilution of the same mouse monoclonal antibody and detected with a 1:2,500 dilution of a horseradish peroxidase-conjugated goat α-mouse antiserum together with the ECL kit (Amersham Pharmacia Biotech, Buckinghamshire, UK).

Image processing. All histology preparations were visualized on a Leitz orthoplan microscope. Photographs were obtained using the Improvision Open-Lab Users Software program (Quincy, MA).

Statistics. Values are means ± SE ($n = 3$–10). Differences were compared using a *t*-test, and $P \leq 0.5$ was considered significant.

RESULTS

Mouse GGT mRNA subtypes in GGT^{enu1} lung. Primer pairs directed against the common GGT coding domain or the unique 5′-untranslated (UT) domain of GGT P3 generated a PCR signal in the rat lung control,

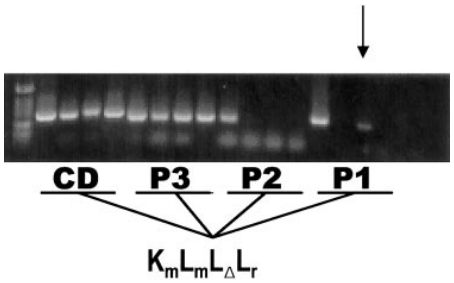

Fig. 1. Expression of γ-glutamyl transferase (GGT) mRNA subtypes in mouse lung. Lung RNA was obtained from normal (L_m) and GGT^{enu1} (L_Δ) mice. RT-PCR was performed as described in METHODS. Primers were selected to target the common coding domain (CD) to detect expression of any GGT mRNA transcript and the specific 5′-untranslated domains to detect expression of the specific GGT mRNA transcript derived from alternative use of promoters P3, P2, or P1. PCR products were separated on a 1.5% agarose gel, visualized with ethidium bromide, and photographed under ultraviolet light. Normal mouse kidney (K_m) was used as a positive PCR control, since all 3 GGT mRNA subtypes are expressed in this organ. Results were compared with normal rat lung (L_r). Arrow, presence of PCR product for GGT P1 in mutant lung RNA.

the mouse kidney control, and the lungs of wild-type and mutant GGT^{enu1} mice (Fig. 1). Those directed at the 5′-UT domain of GGT P2 generated a product only in the mouse kidney control. However, primers for the 5′-UT domain of GGT P1 generated product in the mouse kidney control and the GGT^{enu1} mouse lung, whereas no product was evident in the normal mouse lung or the rat lung. This pattern of GGT P1 mRNA expression in GGT^{enu1} mouse lung matches the pattern we previously described in the oxidant-exposed rat lung (36) and suggests that the GGT^{enu1} mouse lung is sensing an oxidant stress even in normoxia.

Lung glutathione content. To further explore the nature of this stress, we measured total glutathione content in plasma, lung, lung lavage, and lung bronchoalveolar lavage (BAL) cells in GGT^{enu1} mice and compared these values with values in normal control mice (Table 1). Total glutathione levels in the plasma were elevated fourfold in GGT^{enu1} mice, in agreement with the previous report in the literature (15). However, total glutathione content of the GGT^{enu1} lung was only minimally reduced from that of the normal controls, and the total glutathione content of the lung ELF was actually elevated nearly twofold in GGT^{enu1} mice. Although these two results do not suggest oxidant stress, the fraction of GSSG was increased more than threefold in the GGT^{enu1} lung and fourfold in the GGT^{enu1} ELF.

We then examined the lung cells obtained by BAL. Total glutathione content was decreased sixfold in cells from GGT^{enu1} lung compared with normal control lung, and this decrease was coupled with a sevenfold increase in the fraction of GSSG. The yield of cells obtained from a single lavage was increased from 137 ± 68 × 10^3 per normal lung (n = 8) to 237 ± 34 × 10^3 per GGT^{enu1} lung when corrected for body weight (n = 6, $P < 0.5$). Differential cell counts showed 99% of the cells to be alveolar macrophages. Hence, oxidant stress is evident by increased levels of GSSG and alterations in glutathione homeostasis in the whole lung, the lung lining fluid, and the alveolar macrophage population of the GGT-deficient GGT^{enu1} lung.

Nonciliated cells in the bronchioles (Clara cells) of normal adult lung express high levels of GGT (9, 27, 29). Hence, GGT deficiency could predispose to glutathione deficiency in these cells. We used an immunohistochemical technique to assess glutathione content in these cells in situ, since highly purified populations of freshly isolated Clara cells cannot be readily obtained from the lung, and the prolonged isolation procedure itself could alter cellular glutathione content. Because an ex vivo biochemical assay of liver glutathione has already shown that glutathione content in the GGT^{enu1} liver is only 30% of that in the normal liver (15), we analyzed this organ first and confirmed that our immunohistochemical technique detects a difference in the glutathione signal between GGT^{enu1} and normal hepatocytes. The signal intensity in the liver, when calibrated, did indicate a 4.7-fold decrease in glutathione content in GGT^{enu1} hepatocytes (175 μM) compared with normal cells (830 μM; Fig. 2). When we applied this technique to the lung, a difference in glutathione content was evident, specifically in the nonciliated cells in the bronchiolar epithelium. In normal lung, a glutathione signal was present in ciliated and nonciliated bronchiolar epithelial cells, but it was more intense in the ciliated cells. In GGT^{enu1} lung, an intense glutathione signal was still present in the ciliated cells, but it was very weak in the nonciliated cells, reflecting a decrease in glutathione content in the subset of bronchiolar epithelial cells that normally express high levels of this ectoenzyme. Much lower levels of GGT are expressed in alveolar epithelial type II than in Clara cells, and differences in glutathione

Table 1. *Glutathione content*

	Plasma	Lung		Lung Lining Fluid		Alveolar Macrophages	
Genotype	Total GSH, μM	Total GSH, nmol/mg protein	%GSSG	Total GSH, μM	GSH/GSSG	Total GSH, nmol/10^6 cells	%GSSG
+/+	61 ± 2.4 (6)	0.80 ± 0.12 (10)	9 ± 1 (6)	834 ± 190 (4)	6.9 ± 0.2 (3)	5.1 ± 1.0 (9)	10 ± 2 (9)
−/−	265 ± 52* (3)	0.76 ± 0.15 (5)	31 ± 2* (6)	1,639 ± 164* (3)	3.3 ± 0.26* (3)	0.88 ± 0.55* (5)	70 ± 6* (5)

Values are means ± SE of number of determinations in parentheses. +/+, Normal mice; −/−, GGT^{enu1} mice (a genetic model of γ-glutamyl transaminase deficiency); GSH, glutathione; GSSG, oxidized glutathione. *Significantly different from +/+ ($P < 0.05$, t-test).

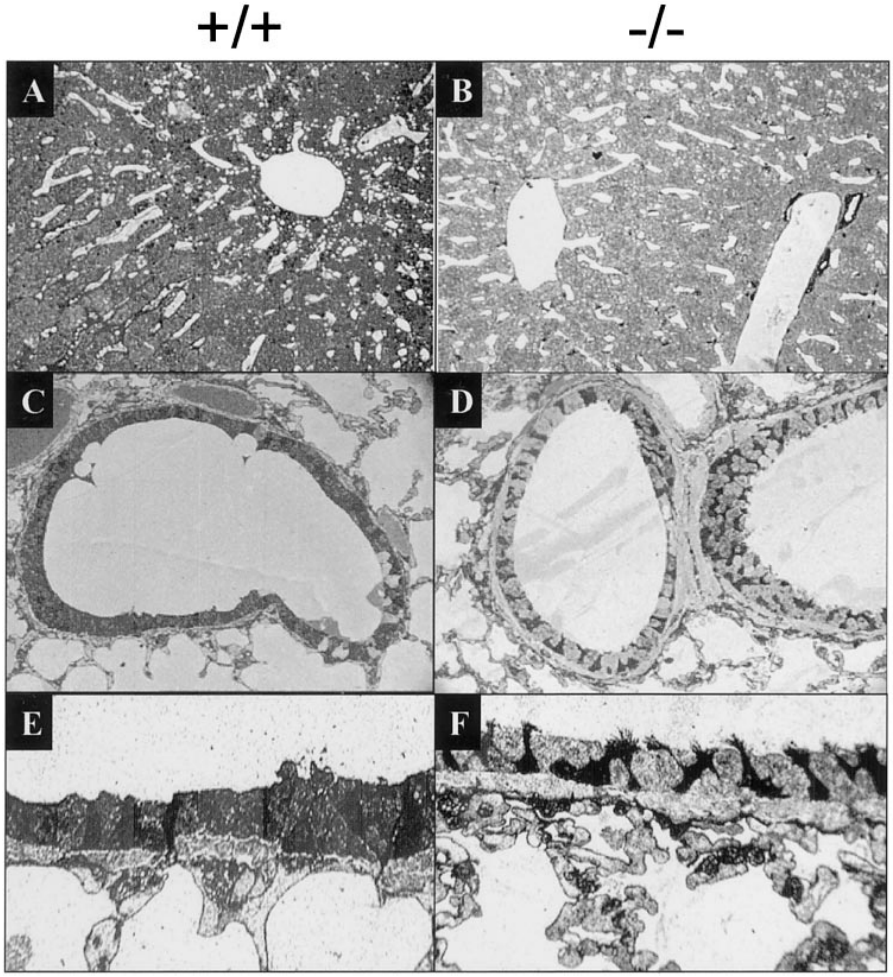

Fig. 2. Detection of glutathione in lung bronchiolar epithelial cells by immunohistochemistry. Liver and lung tissues from normal (+/+) and GGT^{enu1} (−/−) mice were fixed, embedded, sectioned, and processed for glutathione immunohistochemistry using a silver enhancement technique. The difference in glutathione signal intensity between +/+ (*A*, ×40x) and −/− (*B*, ×40) liver suggested a 4.7-fold decrease in glutathione content in hepatocytes of GGT^{enu1} mice. Signal from bronchiolar epithelium of normal lung is shown in *C* (×40) and *E* (×100) and from GGT^{enu1} lung in *D* (×40) and *F* (×100). Black signal from normal lung is dense in ciliated cells (cilia are not very well preserved in this section) and less so in nonciliated cells. In contrast, this signal in the GGT^{enu1} lung remains dense in ciliated cells but is very pale in nonciliated cells, indicating glutathione depletion.

content were not evident in these GGT^{enu1} cells (data not shown).

Nitrotyrosine immunoreactivity. Because the glutathione immunohistochemical signal could not distinguish between the relative content of reduced and oxidized glutathione, we probed for 3-nitrotyrosine as described in METHODS to determine whether glutathione deficiency in the GGT^{enu1} bronchioles was associated with cellular oxidant stress. These modified tyrosine residues result from the interaction of tyrosine with peroxynitrite and are stable products (18). A 3-nitrotyrosine signal was evident in some bronchiolar cells of normal lung, but it was weak and sparse. In contrast, this signal was more intense and diffuse in the bronchiolar epithelium of GGT^{enu1} lung (Fig. 3). A nitrotyrosine signal was also evident in glutathione-depleted alveolar macrophages from the GGT^{enu1} lung (data not shown). The nitrotyrosine signal was inhibited by coincubation of primary antibody with 10 mM nitrotyrosine to ensure specificity of the signal. The decreased glutathione content in concert with the increased nitrotyrosine signal indicates the presence of increased oxidant stress in nonciliated bronchiolar epithelial cells in the GGT^{enu1} lung.

Survival in normobaric hyperoxia. Because the alterations in the pattern of lung GGT mRNA expression, lung glutathione homeostasis, and 3-nitrotyrosine immunocytochemistry suggested the presence of oxidant stress even in normoxia, we hypothesized that GGT^{enu1} mice would be more sensitive than their normal controls to an inhaled oxidant stress. To determine this, we exposed them to an atmosphere of >95% O_2 and measured survival as described in METHODS. At the outset, no major differences in the lung parenchyma were apparent between the two groups on the basis of histological criteria. However, survival of GGT^{enu1} mice was reduced ~25% compared with their normal controls (Fig. 4).

The reduced survival of the GGT^{enu1} mice in hyperoxia suggested that oxidant stress and injury were accelerated in their lung cells. To examine this, we compared the histological appearance, the expression of HO-1 protein, and the immunohistochemical signal for glutathione content in GGT^{enu1} and normal lungs after 96 h in hyperoxia, since this was the average time

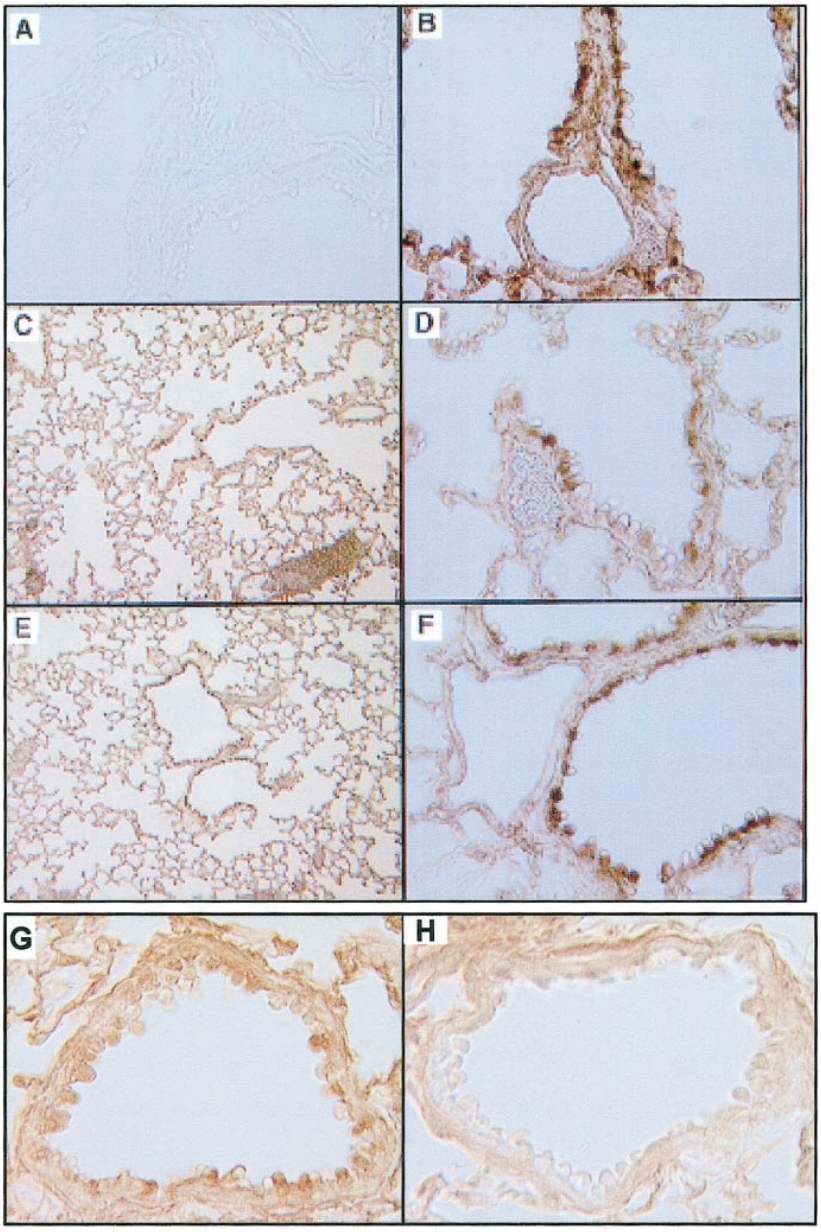

Fig. 3. Detection of immunoreactivity for 3-nitrotyrosine. To determine the presence of oxidant stress in bronchiolar epithelium, 3-nitrotyrosine, the stable end product of the interaction of peroxynitrite with cellular tyrosine residues, was immunolocalized in lung tissue. *A*: GGT^{enu1} lung was incubated with nonimmune serum as a negative control. *B*: normal lung was preincubated with 1 mM exogenous peroxynitrite before exposure to polyclonal rabbit α-nitrotyrosine antibody as a positive control. Normal (*C* and *D*, ×100) and GGT^{enu1} (*E* and *F*, ×200) lungs were incubated with the same antiserum. To ensure specificity of the 3-nitrotyrosine signal, GGT^{enu1} lung was coincubated with the same antiserum in the absence (*G*) or presence (*H*) of 10 mM nitrotyrosine.

of death for the mutants. At this time point, histology revealed well-developed and prominent perivascular edema and bronchiolar epithelial cell injury and disruption in the GGT^{enu1} lung, whereas there was little evidence of this in the normal lung (Fig. 5). In normal lung, HO-1 protein, a marker of oxidant stress, immunolocalized only to the alveolar macrophage in normoxia, as noted by others (6), and after 96 h in hyperoxia, extended to include vascular endothelial, but not epithelial, cells. This contrasts with the GGT^{enu1} lung, where endothelial cell HO-1 expression was already evident in lung vasculature even in normoxia, as it was in GGT^{enu1} liver, which was examined as a positive control for HO-1 expression. No HO-1 signal was detected in any epithelial cells of the GGT^{enu1} lung in normoxia, but, after 96 h in hyperoxia, HO-1 protein expression extended widely throughout the airway and the alveolar epithelium (Fig. 6).

This induction of HO-1 protein was confirmed with a Western blot using the same monoclonal antibody. Exposure to hyperoxia induced this protein in the lungs of GGT^{enu1} and normal mice, but the HO-1 signal was more intense in GGT^{enu1} lung not only at 96 h of hyperoxia but also in the basal state under normoxia. The 31-kDa mouse HO-1 protein as well as the 32-kDa rat HO-1 protein control migrated more rapidly under our electrophoresis conditions than predicted from the calculated molecular mass (Fig. 7).

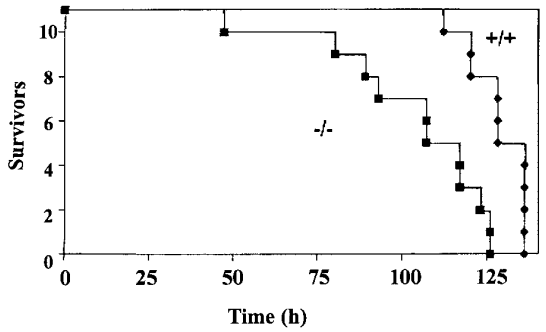

Fig. 4. Survival curve in normobaric hyperoxia. Eleven GGT^{enu1} (−/−) and 11 normal (+/+) mice were exposed to >95% O_2. Survival times were 103 ± 24 and 129 ± 8 h for GGT^{enu1} and normal mice, respectively. Values are means ± SD (P = 0.003 by t-test).

Next, we assessed cellular glutathione content after 96 h in hyperoxia using immunohistochemistry. The glutathione signal in the normal lung remained intense in bronchiolar epithelial cells and cells within the parenchyma of the lung that may represent alveolar epithelial type II cells. In contrast, the intensity of the glutathione signal in the cells of the mutant lung was dramatically decreased compared with that in the normal lung after 96 h in hyperoxia. This was evident in airway epithelial cells, cells within the lung parenchyma, and the alveolar lining itself (Fig. 8). The mutant lung, in contrast to the normal lung, also exhibited patches of cells where the glutathione signal was more preserved, suggesting that certain regions were more metabolically challenged than others. Overall, on exposure to hyperoxia, glutathione depletion developed more rapidly in the GGT^{enu1} than in the normal lung.

Finally, perimortem histological examination of the GGT^{enu1} lung in hyperoxia revealed extensive airway epithelial cell injury, especially in the bronchioles, and intense perivascular edema together with alveolar cell damage and hemorrhage. Although this was also evident in the normal lung, these findings were more prominent in the GGT^{enu1} lung (Fig. 9).

DISCUSSION

GGT is the key enzyme that initiates the metabolism and turnover of glutathione. The metabolic function of this cell surface glycoprotein is believed to protect the plasma membrane against oxidant stress and to enable the transfer of glutathione between cells and tissues. GGT is most abundant in epithelial cells and their secretions, inasmuch as these cells line surfaces that

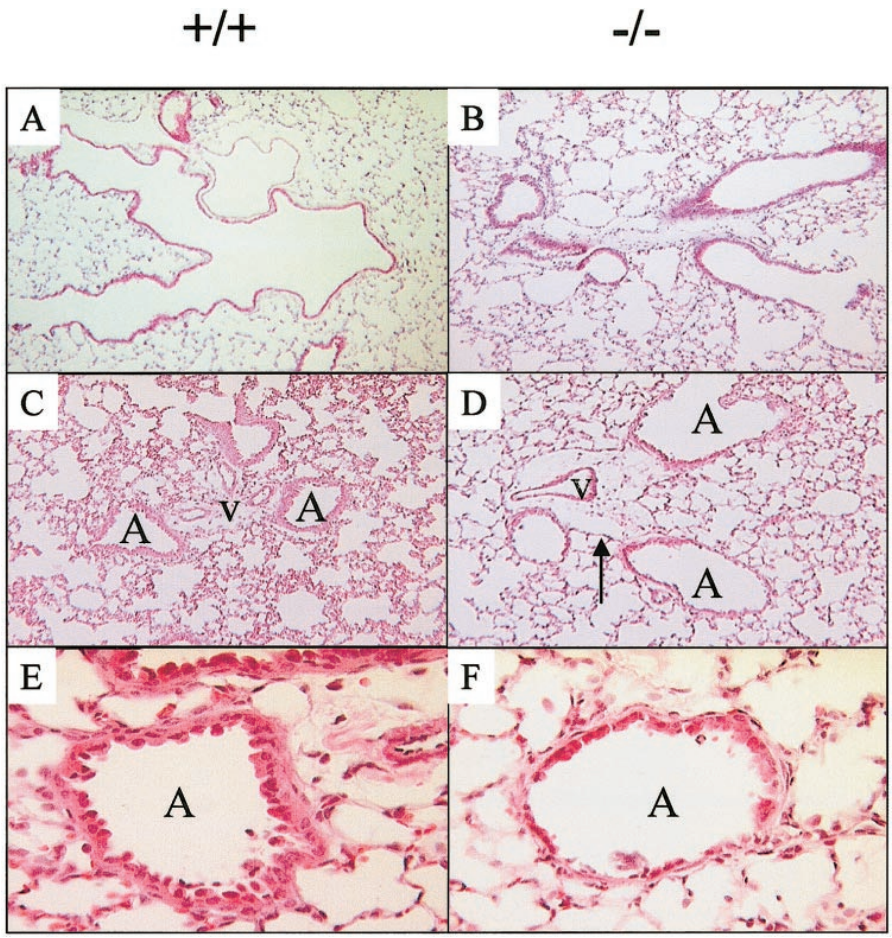

Fig. 5. Histological comparison of normal (+/+) vs. GGT^{enu1} (−/−) lung after 96 h in hyperoxia. Lung tissue from normal and GGT^{enu1} mice was fixed, embedded, sectioned, stained, and photographed. Normal lung is shown under normoxic conditions in A and after 96 h of exposure to >95% O_2 in C (×10) and E (×40). GGT^{enu1} lung is shown under normoxic conditions in B and after a similar exposure to hyperoxia in D (×10) and F (×40). A, airway; V, blood vessels; arrow, perivascular edema.

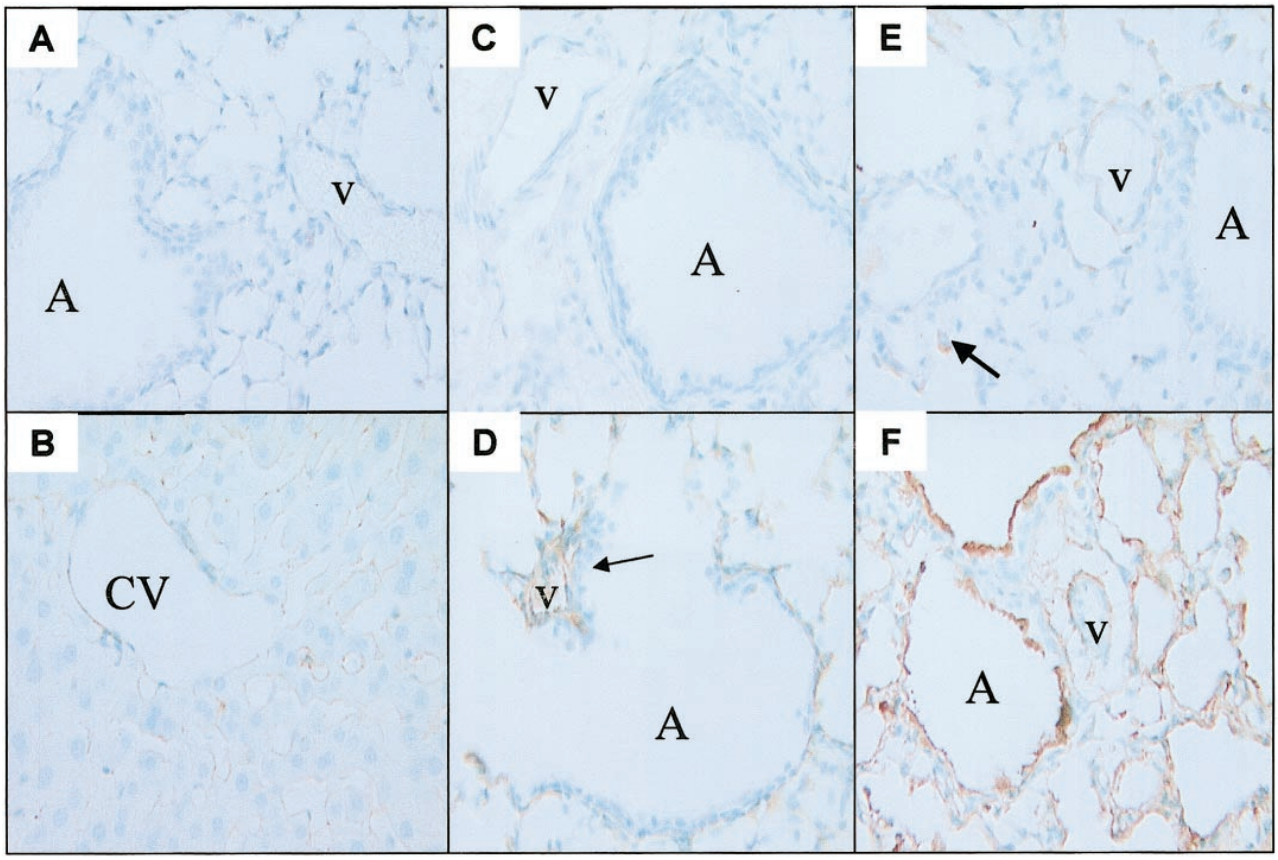

Fig. 6. Histological comparison of heme oxygenase-1 (HO-1) expression in normal vs. GGT^{enu1} lung after 96 h in hyperoxia. Lung tissue from normal and GGT^{enu1} mice was fixed, embedded, sectioned, and probed for HO-1 protein. Primary antibody was omitted during processing of GGT^{enu1} lung sample in *A* as a negative control, and no signal (brown color) is evident. GGT^{enu1} liver was probed in *B* as a positive control, and brown signal is evident along hepatic sinusoids (CV, central vein). Normal lung is shown under normoxic conditions in *C* and after 96 h of hyperoxia in *E* (arrow, signal in alveolar macrophage in normal lung). The same is shown for GGT^{enu1} lung in *D* (arrow, signal in blood vessel from mutant lung) and *F*. A, airways; V, blood vessels. Magnification ×40.

are directly exposed to environmental oxidants. We have demonstrated in the lung that GGT is expressed highly in Clara cells of the bronchioles and, to a lesser degree, in type II cells in the alveolus. We have also shown that GGT activity accumulates in surfactant secretions of the normal lung. The lung responds to oxidant gas exposure by inducing the GGT gene in epithelial cells and accumulating enzyme activity in surfactant secretions. This leads to an acceleration of glutathione turnover. Although controversy has surrounded the role of GGT in the lung, our studies have led us to propose that GGT-mediated glutathione metabolism serves a critical antioxidant function at the epithelial surface of the distal lung (22, 36).

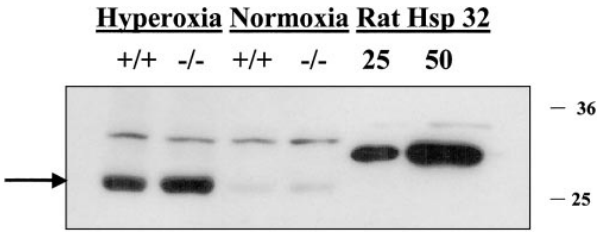

Fig. 7. Comparison of HO-1 protein expression in normal vs. GGT^{enu1} lung in normoxia and after 96 h in hyperoxia. Total protein was extracted from normal and GGT^{enu1} lung after 96 h in hyperoxia or normoxia, separated on a 10% polyacrylamide gel, transferred to a nitrocellulose filter, and probed for expression of HO-1. Twenty-five and 50 μg of rat HO-1 [heat shock protein 32 (HSP32)] were loaded for comparison, and this standard, along with the 31-kDa mouse protein (arrow), exhibited an anomalous pattern of migration in our gel system. Molecular weight standards are marked for 36,000 and 25,000 at *right*.

To study this further, we initially characterized the point mutation that inactivated the GGT gene in the GGT^{enu1} mouse and presented evidence that the GGT^{enu1} kidney was under oxidant stress in normoxia (15, 19). We have compared the lungs of normal and GGT^{enu1} mice in normoxia, and we demonstrate oxidant stress at critical sites where GGT expression is lost. These findings correlate well with our previous results on the localization of lung GGT expression. The GGT^{enu1} lung exhibits a deficiency of glutathione in the bronchiolar Clara cell and a disruption of glutathione homeostasis in the ELF that lead to glutathione defi-

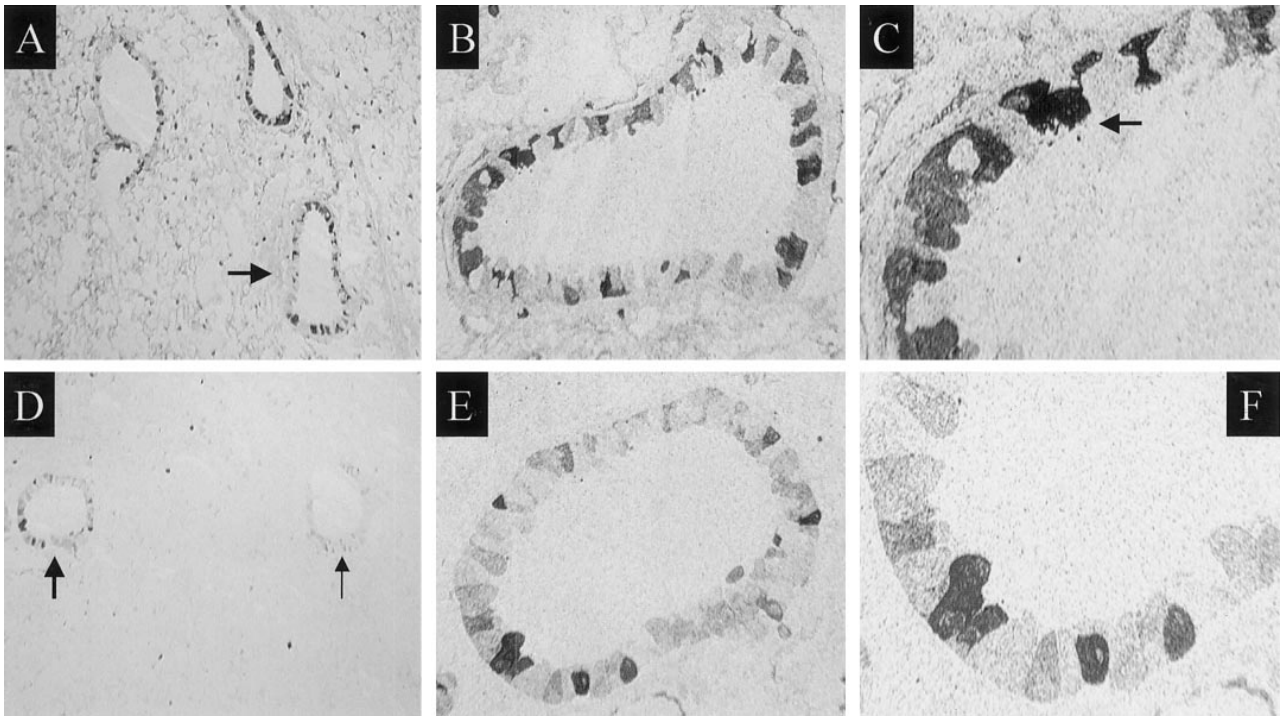

Fig. 8. Comparison of lung glutathione content in normal vs. GGT^{enu1} lung after 96 h in hyperoxia. Lung tissue from normal (*A–C*) and GGT^{enu1} (*D–F*) mice was harvested, fixed, and assayed for glutathione content as described in Fig. 2 legend. All glutathione signals are lower in GGT^{enu1} than in normal lung. A low-power view (×10) shows small bronchioles from normal (*A*) and GGT^{enu1} (*D*) lung. Arrow in *A* denotes normal bronchiole shown at ×40 (*B*) and ×100 (*C*, arrow points to ciliated cell). Normal lung airway epithelium still exhibits an intense signal, as do many parenchymal lung cells and the very thin alveolar lining. In contrast, the glutathione signal is much more uneven and pale in GGT^{enu1} bronchioles (thin arrow) and parenchyma, suggesting generalized glutathione depletion. However, the signal was patchy, with some bronchioles (thick arrow) exhibiting a more preserved signal as shown at ×40 (*E*) and ×100 (*F*). This serves as an internal control for the method and suggests that some bronchioles in the GGT^{enu1} lung are more metabolically challenged than others.

ciency in the alveolar macrophage. We also found that the vascular endothelium is under oxidant stress in normoxia as HO-1 protein is induced in these cells. This stress in the vasculature may originate from the loss of GGT expression on the endothelial cell surface, inasmuch as these cells are known to express GGT at a very low level, or from the plasma, inasmuch as a pool of GGT circulates in the blood (30). The consequences of oxidant stress in the GGT^{enu1} lung become manifest when the mutant mice are exposed to hyperoxia. The formation of pulmonary edema and hemorrhage are accelerated as a result of vascular injury. Glutathione deficiency and oxidant stress extend widely throughout the epithelial surface. Epithelial cell injury and disruption, which predominate in the bronchioles, lead to air space edema and hemorrhage. Hence, survival of the GGT^{enu1} mice in hyperoxia is decreased compared with the normal control mice. The degree of O_2 sensitivity that we observed in the GGT^{enu1} lung is similar to that which occurs with inactivation of the extracellular superoxide dismutase gene, the enzyme activity of which clears superoxide radicals from the extracellular environment (5).

Despite the presence of oxidant stress in the GGT^{enu1} lung, there is only a minimal decrease of total glutathione in this organ. This contrasts with the GGT^{m1}/GGT^{m1} mouse, a model of GGT deficiency produced by targeted mutagenesis of the GGT gene. The GGT^{m1}/GGT^{m1} mouse model differs from the GGT^{enu1} mouse as follows: *1*) there is no detectable GGT activity in GGT^{m1}/GGT^{m1} mice, *2*) the degree of glutathionuria is more profound, and *3*) there is an absolute deficiency of plasma cysteine. Because cysteine supply is critical for glutathione synthesis, a deficiency of glutathione is evident in many GGT^{m1}/GGT^{m1} organs, including the lung (24, 34). GGT^{m1}/GGT^{m1} mice are reportedly sensitive to even 80% O_2, usually a sublethal level of O_2, indicating that the lung glutathione deficiency is probably severe and generalized. Exogenous cysteine replacement restores glutathione content in the lung as a whole and eliminates the sensitivity to this level of hyperoxia (3).

The GGT^{enu1} mouse model of GGT deficiency was produced by inducing random mutations in the mouse genome with ethylnitrosourea (enu) and then selecting progeny for the presence of aminoaciduria, which was glutathionuria in the GGT^{enu1} mouse. GGT gene expression was inactivated; yet a small residuum of GGT activity persisted in the kidney (15). As a result, the degree of glutathionuria was less profound, and

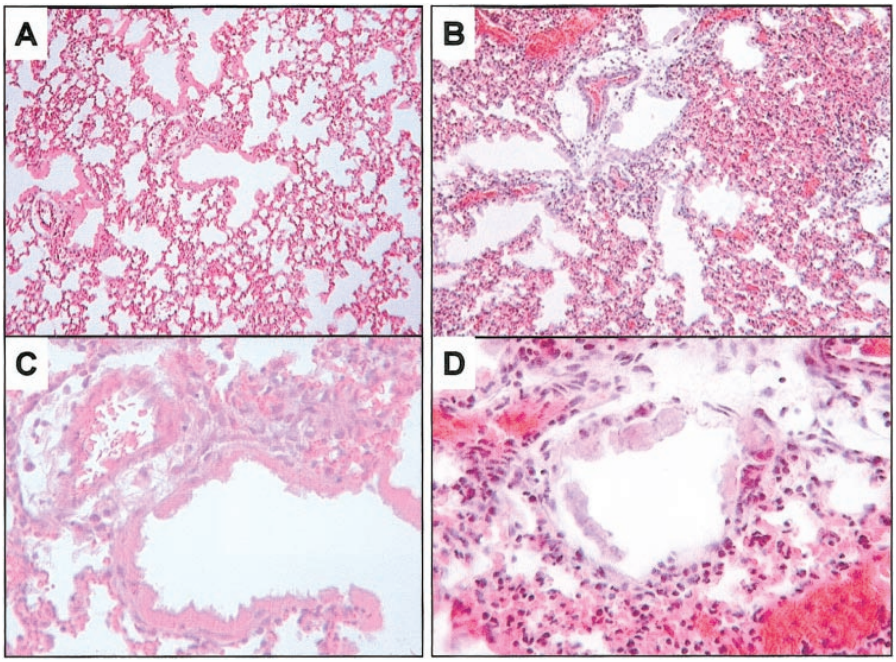

Fig. 9. Perimortem histological comparison of normal vs. GGT^{enu1} lung exposed to hyperoxia. Lung tissue from normal and GGT^{enu1} mice was fixed immediately at the time of death, embedded, sectioned, and stained. Normal lung is shown in *A* (×10) and *C* (×40) and GGT^{enu1} lung in *B* (×10) and *D* (×40).

plasma cysteine levels were not decreased. Hence, the nearly normal lung glutathione content in normoxia likely reflects the adequacy of the plasma cysteine supply. However, the more than threefold rise in GSSG content in the GGT^{enu1} lung indicates oxidant stress. This stress likely resided within a subset of lung cells where glutathione homeostasis is dependent on GGT.

The activity of GGT P1 as well as P3 in the GGT^{enu1} mouse lung was our initial evidence for oxidant stress in normoxia. In our previous studies in the rat lung, we showed that GGT P3, but not P2 or P1, is active in normal lung. However, GGT P1 is induced after exposure to an inhaled oxidant gas (36). GGT P1 is also developmentally regulated in the perinatal rat lung, a time when oxidant stress is also believed to occur (29). Because the genomic organization of the GGT gene is highly conserved between the rat and the mouse (7), GGT P3, but not P2 or P1, activity in the normal mouse lung was the expected result and confirms that described in the literature (13). The activity of GGT P1 solely in the GGT^{enu1} lung suggests that the GGT-deficient lung is under oxidant stress. GGT P1 is the most proximal promoter in the rat and the mouse GGT gene, and its activation in response to oxidant stress appears to be a common response in both species. We suspect that GGT P1 is active in the bronchiolar Clara cell, since we have shown that this cell is the major site of GGT gene expression in the distal lung (29, 36). Current work is focused on confirming this hypothesis and determining the oxidant-associated mechanism of GGT P1 activation.

The loss of GGT gene expression in the lung correlates specifically with a cellular deficiency of glutathione in the subset of nonciliated bronchiolar epithelium (Clara cells). These cells are located in small airways that are prone to injury from inhaled particulates and oxidants, and glutathione export and GGT-mediated recycling may be important to protect their plasma membrane against oxidative damage (28). GGT deficiency could predispose to glutathione depletion in these cells in two ways. Uncoupling glutathione export from metabolism could cause glutathione depletion, inasmuch as cellular reuptake of intact glutathione is inefficient (12). Alternatively, Clara cells are also sites of active xenobiotic metabolism, and this function can deplete glutathione stores if utilization exceeds supply. Loss of GGT activity could impair the transfer of glutathione from the ELF into the Clara cell by limiting the supply of cysteine and compromising intracellular glutathione synthesis. In either case, we are examining these cells in the GGT^{enu1} lung to understand the full impact of GGT deficiency on Clara cell biology and function.

That these glutathione-deficient cells are sensing oxidant stress is strongly supported by their intense signal for 3-nitrotyrosine. Even sporadic Clara cells in the normal lung exhibit a signal for 3-nitrotyrosine. This suggests that glutathione stores are very dynamic in this cell. The consequence of this Clara cell glutathione depletion and oxidant stress for the GGT^{enu1} lung became manifest on exposure of the these mice to hyperoxia, whereupon these cells became injured and disrupted more rapidly than the normal Clara cells. This result is intriguing, given that these cells are naturally deficient in GGT at the time of birth, inasmuch as Clara cell GGT ontogeny occurs during the late postnatal period (29). We are now examining the response of the normal and GGT^{enu1} lung to different O_2 environments at birth. Finally, the immunologic signal for glutathione in the population of other cells of

the bronchiole, the ciliated epithelial cell, is the most intense that has been observed with this methodology. There is not a dramatic difference in signal intensity between ciliated cells in the normal and the GGT^{enu1} lung. We do not know the mechanism by which the GGT^{enu1} ciliated bronchiolar cells are able to maintain their glutathione content under normoxia. In hyperoxia, however, glutathione depletion still occurs more rapidly in these cells than in their normal controls.

The alveolar epithelial type II cell also expresses GGT mRNA and protein, although the level of expression is much lower than that of the Clara cell. The type II cell also has abundant glutathione (10) and appears to be the major cellular source of the glutathione that is exported into the lung ELF (17, 26). Despite this export function, our assays for glutathione and 3-nitrotyrosine did not reveal evidence of glutathione depletion or oxidant stress in the GGT-deficient type II cell. The reason for this is not clear. Experiments by others have suggested a correlation between type II cell glutathione export and the extracellular redox state, so that a more oxidized extracellular environment forces the cell to retain glutathione (38). The exact mechanism for this response is unknown, but the presence of oxidant stress in the ELF could have blocked glutathione export from the type II cell and prevented severe glutathione depletion. Alternatively, type II cell glutathione content may have been preserved by the ability of this cell to transport intact glutathione from the ELF via an Na^+-dependent transport process (14).

We showed previously that the type II cell releases GGT activity along with its surfactant secretions (22). Given that the GGT specific activity in this surfactant-associated pool is about sevenfold higher than that of the whole lung, we suspected that GGT deficiency would have a greater impact on the glutathione pool within the ELF. The lung ELF is unique in its glutathione abundance, and this extracellular pool functions in antioxidant protection for the entire gas exchange surface (4). Glutathione concentration in the ELF is clearly elevated in the GGT^{enu1} lung, and this increase would correlate with the absence of glutathione metabolism and clearance by surfactant-associated GGT. Decreased clearance from the blood is believed to be the mechanism of glutathionemia as well (15, 24). However, there was a disproportionate rise in ELF GSSG content in the GGT^{enu1} lung, suggesting that GSSG clearance may have been affected to a greater degree than glutathione clearance. The mechanism by which GSSG is cleared from the alveolar space is unknown, but as a result of its accumulation, the redox state of ELF in the mutant mouse was shifted toward a more oxidized state, even in normoxia. It is known that when the normal lung is chronically exposed to an inhaled oxidant gas, GSSG levels in the ELF rise initially and then return to baseline (23). This suggests the existence of an inducible mechanism that can increase lung GSSG clearance. Studies of GGT activity in the lining fluid of the epididymis suggest that the mechanism is the preferential metabolism of GSSG by GGT protein itself and that this protein serves to regulate the redox state in testicular lining fluid (16). We believe that a similar process may occur in the lung ELF. Although the expanded ELF glutathione pool could have protected the distal lung from oxidant stress in hyperoxia, we did not observe this. Rather, there was a more pronounced depletion of glutathione and induction of HO-1 protein throughout the epithelial surface. Glutathione depletion could have resulted from a dilution by edema fluid or from increased permeability due to the loss of epithelial barrier function with injury in hyperoxia.

The alveolar macrophage is a second subset of lung cells that becomes depleted of glutathione in the GGT^{enu1} lung, despite the expansion of the ELF glutathione pool. Hence, glutathione turnover in the ELF appears to be necessary for glutathione homeostasis within this immune cell. In a previous study, we showed that lung alveolar macrophages do not express GGT mRNA; yet it is known that these cells depend on GGT activity to maintain glutathione homeostasis (11). We proposed that this enzyme activity was derived from lung surfactant, and our results support this hypothesis (22). The level of macrophage glutathione depletion that we observed in the GGT^{enu1} lung in normoxia is severe, and the high content of GSSG indicates intense glutathione utilization. We do not know why there is an increase in the number of alveolar macrophages in the GGT^{enu1} lung or how this severe redox imbalance affects macrophage function. However, preliminary experiments with expression of interleukin-1β, interleukin-converting enzyme, and inducible nitric oxide synthase in GGT^{enu1} macrophages suggest that these cells are not in an activated state, despite the presence of oxidant stress (20). The inability of these immune cells to function optimally could have a negative impact on host defense.

A large body of literature supports the fundamental role of the glutathione system in maintaining normal lung function and protecting against oxidant-induced injury (30). The lung utilizes a large amount of glutathione. In the mouse, it utilizes more glutathione than any other organ (26). Our studies in the GGT^{enu1} mouse show that GGT deficiency has a dramatic impact on glutathione homeostasis and the redox state of the lung. This supports our hypothesis that GGT gene expression serves a critical role in protecting the lung against oxidant stress in normoxia and hyperoxia. The goal of future studies will be to gain a more complete understanding of the function of GGT in the lung and the role of GGT in regulating oxidant stress in specific lung cells. In this regard, we recently showed that GGT and one of its protein isoforms, which are derived from alternative splicing of GGT mRNA, can mediate an endoplasmic reticulum stress response (21). Therefore, in addition to affecting glutathione recycling and the cellular redox state, GGT may serve additional functions directly within the endoplasmic reticulum. Hence, GGT may have a number of important cellular homeostatic functions. The GGT^{enu1} mouse provides a model from which to gain new insight into the biolog-

ical significance of GGT gene expression for cells of the normal and diseased lung.

The authors thank Dr. M. C. Williams for advice regarding the studies on HO-1.

This work was supported by National Heart, Lung, and Blood Institute Program Project Grant PO1 HL-47049 to M. Joyce-Brady.

REFERENCES

1. **Albert Z, Orlowska J, Orlowska M, and Szewczuk A.** Histochemical and biochemical investigations of γ-glutamyl transpeptidase in the tissues of man and laboratory rodents. *Acta Histochem* 18: S78–S89, 1964.
2. **Bai C, Brown LA, and Jones DP.** Glutathione transport by type II cells in perfused rat lung. *Am J Physiol Lung Cell Mol Physiol* 267: L447–L455, 1994.
3. **Barrios RJ, Shi ZZ, Wiseman AL, Welty SE, Kala G, Balher A, Ou CN, and Lieberman MW.** Role of glutathione in lung injury caused by normobaric hyperoxia (Abstract). *FASEB J* 14: A172, 2000.
4. **Cantin AM, North SL, Hubbard RC, and Crystal RG.** Normal alveolar epithelial lining fluid contains high levels of glutathione. *J Appl Physiol* 63: 152–157, 1987.
5. **Carlsson LM, Jonsson J, Edlund T, and Marklund SL.** Mice lacking extracellular superoxide dismutase are more sensitive to hyperoxia. *Proc Natl Acad Sci USA* 92: 6264–6268, 1995.
6. **Carraway MS, Ghio AJ, Carter JD, and Piantadosi CA.** Expression of heme oxygenase-1 in the lung in chronic hypoxia. *Am J Physiol Lung Cell Mol Physiol* 278: L806–L812, 2000.
7. **Chikhi N, Holic N, Guellaen G, and Laperche Y.** γ-Glutamyl transpeptidase gene organization and expression: a comparative analysis in rat, mouse, pig and human species. *Comp Biochem Physiol B Biochem Mol Biol* 122: 367–380, 1999.
8. **Davis WB and Pacht ER.** Extracellular antioxidant defenses. In: *The Lung: Scientific Foundations* (1st ed.), edited by Crystal RG and West JB. New York: Raven, 1991, vol. 2, p. 1821–1827.
9. **Dinsdale D, Green JA, Manson MM, and Lee MJ.** The ultrastructural immunolocalization of γ-glutamyltranspeptidase in rat lung: correlation with the histochemical demonstration of enzyme activity. *Histochem J* 24: 144–152, 1992.
10. **Forkert PG and Moussa M.** Histochemical localization of glutathione in fixed tissues. *Histochem J* 21: 634–637, 1989.
11. **Forman HJ and Skelton DC.** Protection of alveolar macrophages from hyperoxia by γ-glutamyl transpeptidase. *Am J Physiol Lung Cell Mol Physiol* 259: L102–L107, 1990.
12. **Griffith OW and Meister A.** Glutathione: interorgan translocation, turnover, and metabolism. *Proc Natl Acad Sci USA* 76: 5606–5610, 1976.
13. **Habib GM, Carter BZ, Sepulveda AR, Shi ZZ, Wan DF, Lebovitz RM, and Lieberman MW.** Identification of a sixth promoter that directs the transcription of γ-glutamyl transpeptidase type III RNA in mouse. *J Biol Chem* 270: 13711–13715, 1995.
14. **Hagen TM, Brown LA, and Jones DP.** Protection against paraquat-induced injury by exogenous GSH in pulmonary alveolar type II cells. *Biochem Pharmacol* 35: 4537–4542, 1986.
15. **Harding CO, Williams P, Wagner E, Chang DS, Wild K, Colwell RE, and Wolff JA.** Mice with genetic γ-glutamyl transpeptidase deficiency exhibit glutathionuria, severe growth failure, reduced life spans, and infertility. *J Biol Chem* 272: 12560–12567, 1997.
16. **Hinton BT, Pallindino MA, Mattmeuller DR, Bard D, and Good K.** Expression and activity of γ-glutamyl transpeptidase in the rat epididymis. *Mol Reprod Dev* 28: 40–46, 1991.
17. **Holguin F, Moss I, Brown LA, and Guidot DM.** Chronic alcohol abuse impairs alveolar type II cell glutathione homeostasis and function and predisposes to endotoxin-mediated acute edematous lung injury in rats. *J Clin Invest* 101: 761–768, 1998.
18. **Ischiropoulos H.** Biological tyrosine nitration: a pathophysiological function of nitric oxide and reactive oxygen species. *Arch Biochem Biophys* 356: 1–11, 1998.
19. **Jean JC, Harding CO, Oakes SM, Yu Q, Held PK, and Joyce-Brady M.** γ-Glutamyl transferase (GGT) deficiency in the GGT^{enu1} mouse results from a single point mutation that leads to a stop codon in the first coding exon of GGT mRNA. *Mutagenesis* 14: 31–36, 1999.
20. **Joyce-Brady M, Jean JC, Fenton MC, and Liu Y.** GGT deficiency affects the function of epithelial cells in large and small airways and of alveolar macrophages in vivo (Abstract). *Am J Respir Crit Care Med* 163: A839, 2001.
21. **Joyce-Brady M, Jean JC, and Highey RP.** γ-Glutamyltransferase and its isoform mediate an endoplasmic reticulum stress response. *J Biol Chem* 276: 9468–9477, 2001.
22. **Joyce-Brady M, Takahashi Y, Oakes SM, Rishi AK, Levine RA, Kinlough CL, and Hughey RP.** Synthesis and release of amphipathic γ-glutamyl transferase by the pulmonary alveolar type 2 cell. *J Biol Chem* 269: 14219–14226, 1994.
23. **Kawata M, Takahashi Y, and Miura T.** Effects of exposure to nitrogen dioxide and ozone in combination on the activities of the glutathione synthesis enzymes and on the levels of glutathione in rat lungs. *Res Rep Natl Inst Environ Stud Jpn* 115: 163–168, 1988.
24. **Lieberman MW, Wiseman AL, Shi Z, Carter BZ, Barrios R, Ou C, Chevez-Barrios P, Wang Y, Habib GM, Goodman JC, Huang SL, Lebovitz RM, and Matzuk MM.** Growth retardation and cysteine deficiency in γ-glutamyl transpeptidase-deficient mice. *Proc Natl Acad Sci USA* 93: 7923–7926, 1996.
25. **Marc RE.** Mapping glutamatergic drive in the vertebrate retina with a channel permeant organic ion. *J Comp Neurol* 407: 47–64, 1999.
26. **Martensson J, Jain A, Frayer W, and Meister A.** Glutathione metabolism in the lung: inhibition of its synthesis leads to lamellar body and mitochondrial defects. *Proc Natl Acad Sci USA* 86: 5296–5300, 1989.
27. **Martin J, Legg RF, Dinsdale D, and White INH.** Isolation of Clara cells from rat lung using flow cytometry (Abstract). *Biochem Soc Trans* 18: 664, 1990.
28. **Meister A and Anderson ME.** Glutathione. *Annu Rev Biochem* 52: 711–760, 1983.
29. **Oakes SM, Takahashi Y, Williams MC, and Joyce-Brady M.** Ontogeny of γ-glutamyltransferase in the rat lung. *Am J Physiol Lung Cell Mol Physiol* 272: L739–L744, 1997.
30. **Rahman I and MacNee W.** Lung glutathione and oxidative stress: implications in cigarette smoke-induced airway disease. *Am J Physiol Lung Cell Mol Physiol* 277: L1067–L1088, 1999.
31. **Rajagopalan S, Wan DF, Habib GM, Sepulveda AR, McLeod MR, Lebovitz RM, and Lieberman MW.** Six mRNAs with different 5′ ends are encoded by a single γ-glutamyltransferase gene in mouse. *Proc Natl Acad Sci USA* 90: 6179–6183, 1993.
32. **Rennard SI, Basset G, Lecossier D, O'Donnell KM, Pinkston P, Martin PG, and Crystal RG.** Estimation of volume of epithelial lining fluid recovered by lavage using urea as marker of dilution. *J Appl Physiol* 60: 532–538, 1986.
33. **Rishikoff DC, Krupsky M, and Goldstein RH.** The effect of prostaglandin E_2 on cystine uptake and glutathione synthesis by human lung fibroblasts. *Biochim Biophys Acta* 1405: 155–160, 1998.
34. **Rojas E, Valverde M, Kala SV, Kala G, and Lieberman MW.** Accumulation of DNA damage in the organs of mice deficient in γ-glutamyltranspeptidase. *Mutat Res* 447: 305–316, 2000.
35. **Shi ZZ, Habib GM, Lebovitz RM, and Lieberman MW.** Cloning of cDNA and genomic structure of the mouse γ-glutamyl transpeptidase-encoding gene. *Gene* 167: 233–237, 1995.
36. **Takahashi Y, Oakes SM, Williams MC, Takahashi S, Miura T, and Joyce-Brady M.** Nitrogen dioxide exposure activates γ-glutamyl transferase gene expression in rat lung. *Toxicol Appl Pharmacol* 143: 388–396, 1997.
37. **Tate S and Meister A.** γ-Glutamyl transpeptidase: catalytic, structural and functional aspects. *Mol Cell Biochem* 39: 357–368, 1981.
38. **Van Klaveren RJ, Demedts M, and Nemery B.** Cellular glutathione turnover in vitro, with emphasis on type II pneumocytes. *Eur Respir J* 10: 1392–1400, 1997.